

Profilin2 contributes to synaptic vesicle exocytosis, neuronal excitability, and novelty-seeking behavior

Pietro Pilo Boyl^{1,7}, Alessia Di Nardo^{2,7},
Christophe Mulle³, Marco Sassoè-
Pognetto⁴, Patrizia Panzanelli⁴,
Andrea Mele⁵, Matthias Kneussel⁶,
Vivian Costantini⁵, Emerald Perlas¹,
Marzia Massimi¹, Hugo Vara⁴,
Maurizio Giustetto⁴ and Walter Witke^{1,*}

¹EMBL, Mouse Biology Unit, Monterotondo, Italy, ²Childrens's Hospital, Department of Neurology, Boston, MA, USA, ³UMR CNRS 5091, Institut François Magendie, Physiologie Cellulaire de la Synapse, Bordeaux, France, ⁴Department of Anatomy, Pharmacology and Forensic Medicine and Istituto Nazionale di Neuroscienze, University of Turin, Torino, Italy, ⁵Università di Roma 'La Sapienza', Laboratorio di Psicobiologia, Dipart. di Genetica e Biologia Molecolare, Roma, Italy and ⁶Centre for Molecular Neurobiology, ZMNH, University of Hamburg, Hamburg, Germany

Profilins are actin binding proteins essential for regulating cytoskeletal dynamics, however, their function in the mammalian nervous system is unknown. Here, we provide evidence that in mouse brain profilin1 and profilin2 have distinct roles in regulating synaptic actin polymerization with profilin2 preferring a WAVE-complex-mediated pathway. Mice lacking profilin2 show a block in synaptic actin polymerization in response to depolarization, which is accompanied by increased synaptic excitability of glutamatergic neurons due to higher vesicle exocytosis. These alterations in neurotransmitter release correlate with a hyperactivation of the striatum and enhanced novelty-seeking behavior in profilin2 mutant mice. Our results highlight a novel, profilin2-dependent pathway, regulating synaptic physiology, neuronal excitability, and complex behavior.

The EMBO Journal (2007) 26, 2991–3002. doi:10.1038/sj.emboj.7601737; Published online 31 May 2007

Subject Categories: cell & tissue architecture; neuroscience

Keywords: actin binding proteins; neurotransmitter release; profilin2; synaptic actin polymerization

Introduction

The actin cytoskeleton in neurons is a highly dynamic filament system regulating neurite outgrowth and polarity, growth cone motility, dendritic spine motility, as well as neuronal precursor cell migration. Although the actin

*Corresponding author. EMBL, Mouse Biology Unit, Adriano Buzzati-Traverso Campus, Via Ramarini 32, 00015 Monterotondo, Italy.
Tel.: +0039 06 90091 268; Fax: +0039 06 90091 272;
E-mail: witke@embl-monterotondo.it

⁷These authors contributed equally to this work

Received: 21 December 2006; accepted: 3 May 2007; published online: 31 May 2007

cytoskeleton has been shown to play an important role in membrane trafficking events such as vesicle endocytosis and exocytosis (Dillon and Goda, 2005), little is known on the regulatory mechanisms conferred by actin binding proteins. A key molecule for regulating actin dynamics in all cell types is the G-actin binding protein profilin (Carlsson *et al.*, 1977). Genetic studies in yeast, slime molds, fly, and the mouse have confirmed its essential role (Cooley *et al.*, 1992; Balasubramanian *et al.*, 1994; Haugwitz *et al.*, 1994; Witke *et al.*, 2001). Profilins seem to be employed by different actin nucleation complexes such as the Arp2/3 complex (Pollard *et al.*, 2001), the formins (Kovar *et al.*, 2006), and the WAVE-complex (Steffen *et al.*, 2004), although the exact role of profilins in these complexes is not known. The mammalian genome contains four profilin genes, which have diversified in sequence and expression. Profilin3 and profilin4 are restricted to testis (Obermann *et al.*, 2005). Profilin1 is expressed at all stages of embryonic development and in all cell types and tissues (Witke *et al.*, 1998), and deletion of the gene results in a pre-implantation embryonic lethal phenotype (Witke *et al.*, 2001). Profilin2 shows highest expression in the brain (Di Nardo *et al.*, 2000). The role of profilins in brain physiology is not well understood. Experiments in cultured hippocampal neurons (Ackermann and Matus, 2003) and the amygdala of fear conditioned rats (Lamprecht *et al.*, 2006) suggested a postsynaptic function of profilins in dendritic spines stabilization and synaptic plasticity.

To determine the functions of the brain specific profilin we generated mutant mice lacking profilin2. Our results show that profilin2 is required for actin polymerization in the synapse, possibly through a pathway that involves the WAVE-complex. Deletion of profilin2 leads to increased neurotransmitter exocytosis in glutamatergic neurons and hyperactivation of the striatum, which correlates with increased novelty-seeking behavior in the mutant mice. Our data suggest a novel role of profilin2 in controlling vesicle exocytosis and presynaptic excitability.

Results

Overlapping expression of profilin1 and profilin2 in brain and localization to synaptic boutons

Profilin1 and profilin2 are both expressed at substantial levels in the brain, and we have estimated 2- to 3-fold higher levels of profilin2 in brain extracts (Witke *et al.*, 2001). *In situ* hybridization confirmed that profilin1 and profilin2 are broadly expressed in virtually all regions such as the cerebellum, the cortex, the hippocampus, the striatum, and the olfactory bulbs (Figure 1A and B). Significant overlap of expression was also confirmed by quantitative Western blot (see Figure 1B). Only in striatum there seemed to be somewhat less profilin1 protein.

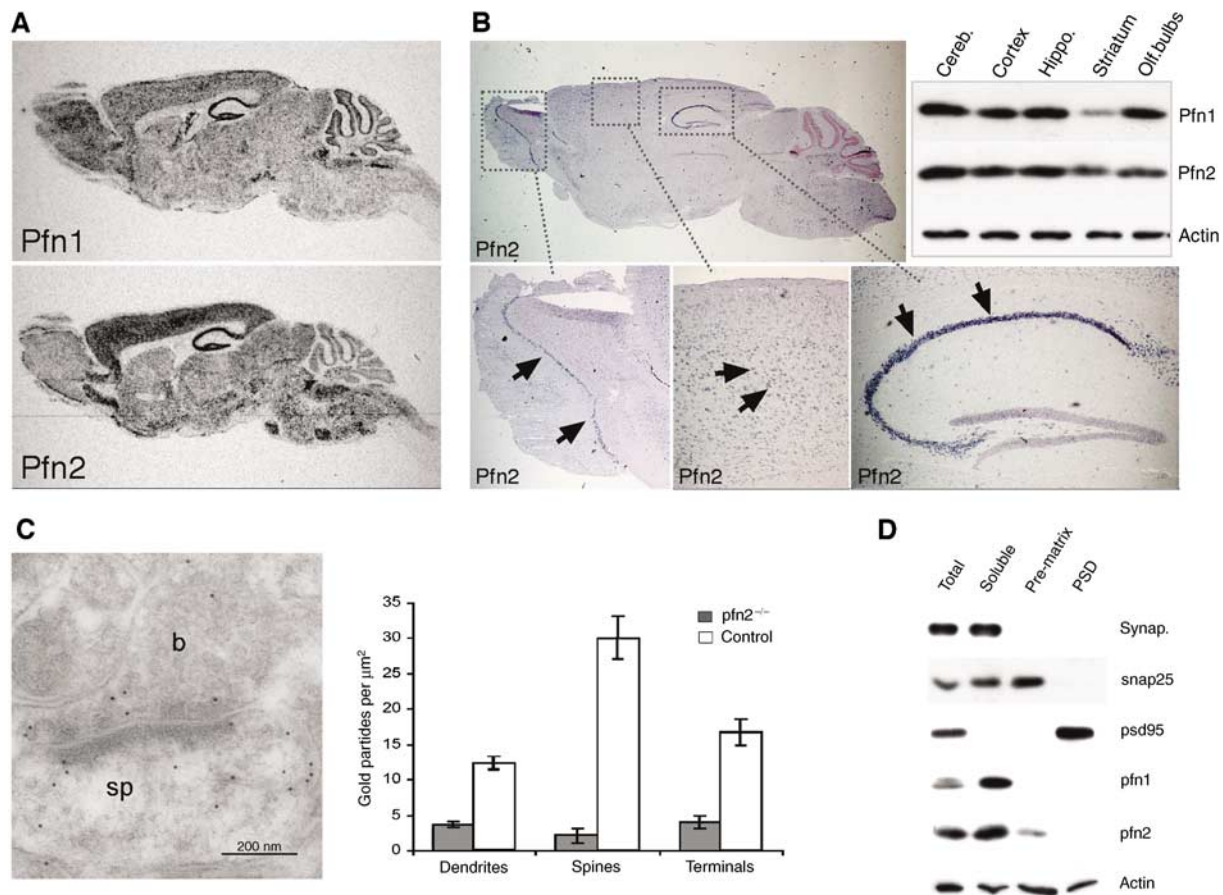


Figure 1 Expression and localization of profilin1 and profilin2 in mouse brain. (A) Radioactive *in situ* hybridization for profilin1 and profilin2 on sagittal sections from adult brains. (B) Profilin2 expression in mitral cells of the olfactory bulb, hippocampal and cortical pyramidal cells (arrows) by non-radioactive *in situ* hybridization. Western blot analysis of profilin1 and profilin2 expression in lysates from dissected brain regions. (C) Immunogold labeling shows profilin2 in the presynaptic bouton (b, left panel) as well as in the postsynaptic spine (sp) of an axospinous synapse of CA1 stratum radiatum. Gold particles were counted in different subcellular compartments of control and $\text{pfn2}^{-/-}$ neurons to account for nonspecific staining ($P < 0.0001$, unpaired *t*-test). (D) Profilin2 distribution in total synaptosomes, the soluble extrasynaptic fraction, presynaptic matrix (pre-matrix), and PSD. Purity of fractions was assessed using the extrasynaptic marker synaptophysin, the presynaptic marker snap25, and the postsynaptic marker psd95. Profilin1 is present in the extrasynaptic fraction, while profilin2 was also found in the presynaptic matrix.

In most non-neuronal cell types profilin1 is sufficient to regulate cytoskeletal dynamics, raising the question what specific requirements of neurons have made a second profilin necessary. The biochemical properties are similar for mammalian profilin1 and profilin2 (Gieselmann *et al*, 1995; Lambrechts *et al*, 1995), but one important difference between profilin1 and profilin2 is their partition in different protein complexes: profilin2 was found with synapsins, dynamin1, (Witke *et al*, 1998), Aczonin/Piccolo (Wang *et al*, 1999) and members of the actin remodeling WAVE-complex (Witke *et al*, 1998), suggesting that profilin2 could play a role in the synapse. Immunogold labeling revealed the presence of profilin2 in both the pre- and the postsynaptic compartments of axospinous synapses (Figure 1C), similar to what has been described for profilin1 (Neuhoff *et al*, 2005). In agreement with the electron microscopy (EM) studies, both profilins were detected in isolated synaptosomes (Figure 1D). Further fractionation of synaptosomes into soluble extrasynaptic content, presynaptic matrix, and postsynaptic density (PSD) showed that most of profilin1 and profilin2 was present in the soluble extrasynaptic fraction. However, profilin2 was reproducibly found associated with the presynaptic matrix, while

under these conditions profilin1 was excluded from this fraction (Figure 1D). Actin was present throughout all synaptosomal fractions, showing that apart from the extrasynaptic actin pool a significant amount of F-actin is tightly bound to the presynaptic matrix and the PSD. The association of profilin2 with the presynaptic matrix and the immunogold localization to boutons and spines would be consistent with a presynaptic as well as a postsynaptic function.

Profilin2 is not essential for neurite extension and neuronal polarization

To address this important issue, we generated knockout mice lacking profilin2 ($\text{pfn2}^{-/-}$ mice, see Supplementary Figure 1A and B). Western blot analysis of $\text{pfn2}^{-/-}$ brain lysates confirmed the absence of profilin2 and normal expression levels of profilin1 (Supplementary Figure 1C). Viable $\text{pfn2}^{-/-}$ mice were born at the expected ratio, indicating that profilin2 is not essential for general embryonic development. More surprising was that the development of the nervous system proceeded normally. Nissl staining of $\text{pfn2}^{-/-}$ and control brains showed no gross differences in brain morphology, such as cortical layering, organization of the hippocampus,

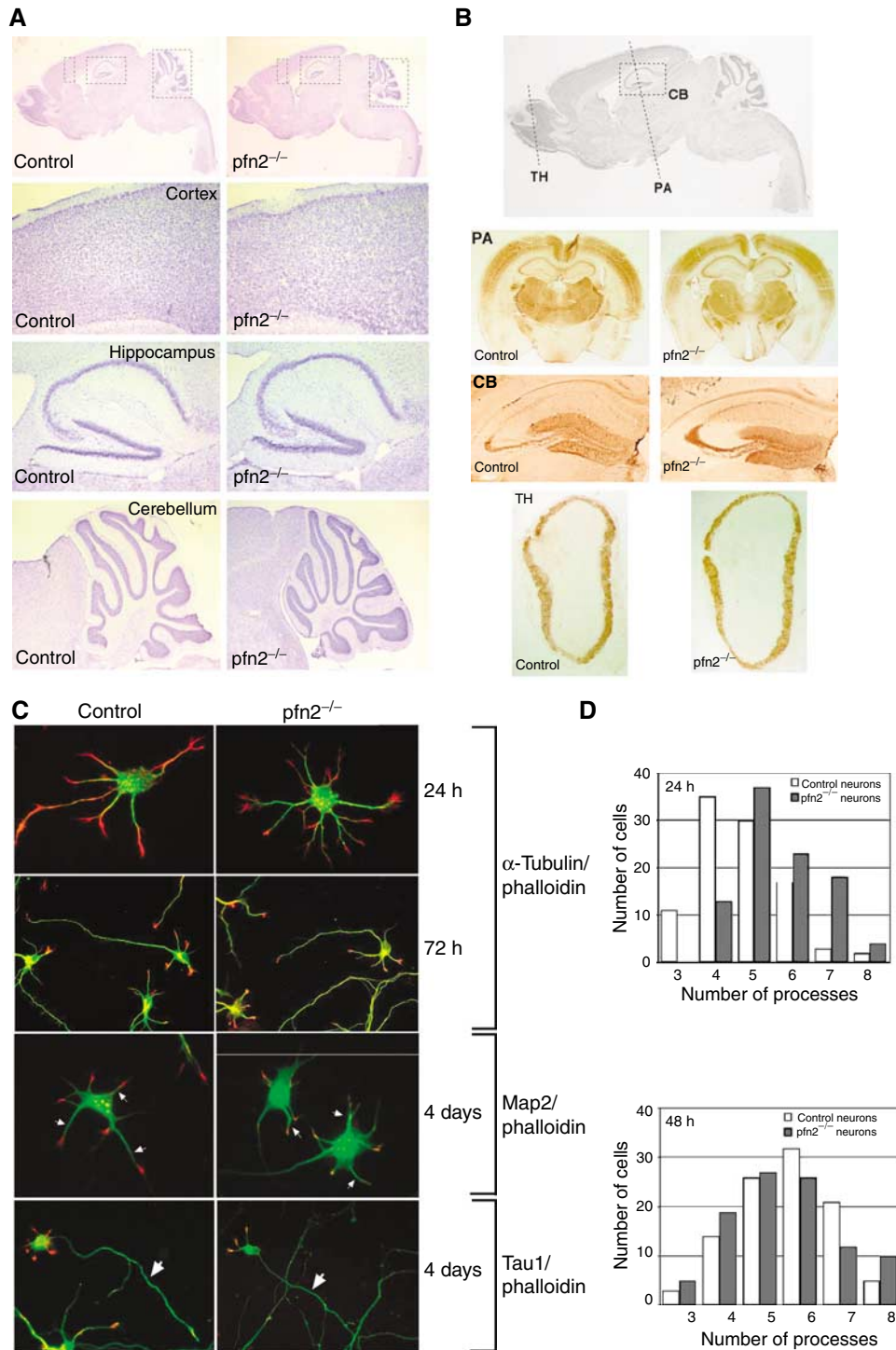


Figure 2 Anatomy of *pfn2*^{-/-} brains and morphology of mutant hippocampal neurons are normal. **(A)** Cresyl violet staining of sagittal sections from control and *pfn2*^{-/-} brains. Overview of sagittal sections (upper), and higher magnifications of the indicated regions from the cortex, the hippocampus, and the cerebellum. **(B)** Immunohistochemistry on *pfn2*^{-/-} and control brains for different neuronal markers. Coronal sections as marked in the sagittal overview (upper) were stained with anti-parvalbumin (PA), anti-calbindin (CB), and anti-tyrosine hydroxylase (TH) antibodies. **(C)** Cytoskeletal organization in cultured hippocampal neurons. Twenty-four hours and 72 h after plating, neurons were fixed and stained for F-actin (TRITC-phalloidin, red) and microtubules (α -tubulin antibody, green). F-actin and microtubules are distributed normally in dendritic and axonal growth cones. Four days after plating, dendritic processes (Map2 staining, green, arrows) and axonal outgrowth (Tau1 staining, green, arrows) were comparable in *pfn2*^{-/-} and control neurons. **(D)** Quantification of dendritic processes. The distribution of cells with a certain number of processes is shown. At least 100 cells were analyzed for each genotype and each time point. After 24 h of culture, *pfn2*^{-/-} neurons showed a small increase in the number of processes, while after 48 h this difference was no longer detectable.

or architecture of the cerebellum (Figure 2A). Immunohistochemical staining with antibodies for specific neuronal markers did not reveal alterations in neuronal subpopula-

tions (Figure 2B). Further ultrastructural analysis confirmed normal synapse number and morphology as shown for the hippocampus, the cerebellum, and the striatum

(Supplementary Figure 2B and Figure 5A and C). These results demonstrate that *in vivo* profilin2 is not required for neuronal migration and differentiation. This was also confirmed in cultured hippocampal neurons, which provide a good model to study the different steps of actin-dependent attachment, spreading, and neurite outgrowth (Bradke and Dotti, 1999). As shown in Figure 2C, neurons from *pfn2*^{-/-} mice followed the normal pattern of attachment, neurite outgrowth, and polarization. No alterations in Map2, Tau1, and F-actin distribution were observed, suggesting that dendrite formation, axonal outgrowth, and growth cone organization were normal in the absence of profilin2. The only difference was observed in the initial spreading of neurons, within the first 24 h after plating. Mutant neurons showed a small increase in the average number of processes per cell (Figure 2D); however, this difference was no longer detectable at 48 h and any later stage. We conclude that profilin2 might play a role in the provision of plasma membrane during spreading, but that profilin2 is not required for actin-dependent neurite outgrowth and development of axonal/dendritic polarity. This was further supported *in vivo* by the normal appearance and presence of all main commissures in *pfn2*^{-/-} mice (Supplementary Figure 2A). It is noteworthy that while complete deletion of profilin2 has

no effect on brain morphology, deletion of a single profilin1 allele (Witke *et al*, 2001) already leads to changes such as an anterior displacement of the hippocampus and a premature resolution of the corpus callosum (see *pfn1*^{+/-}; Supplementary Figure 2A). This alteration is identical in compound mutants, heterozygous for the profilin1 and profilin2 mutation (*pfn1*^{+/-}, *pfn2*^{+/-}), supporting the notion that profilin1 has a function distinct from profilin2.

Profilin2 is not required for LTP/LTD and learning and memory

Since the architecture of *pfn2*^{-/-} brains was normal, we used this mouse model to study the role of profilin2 in neuronal physiology and synaptic activity. Experiments on cultured neurons had suggested a postsynaptic function of profilin2 in dendritic spine stabilization (Ackermann and Matus, 2003), and in rats, recruitment of profilin into spines was observed after fear conditioning (Lamprecht *et al*, 2006). Based on these findings a role of profilin2 in regulating synaptic plasticity has been proposed.

However, by electrophysiology and behavioral experiments, we were not able to detect any postsynaptic impairment or lack of synaptic plasticity in *pfn2*^{-/-} mice. Long-term potentiation (LTP) and long-term depression (LTD) measure-

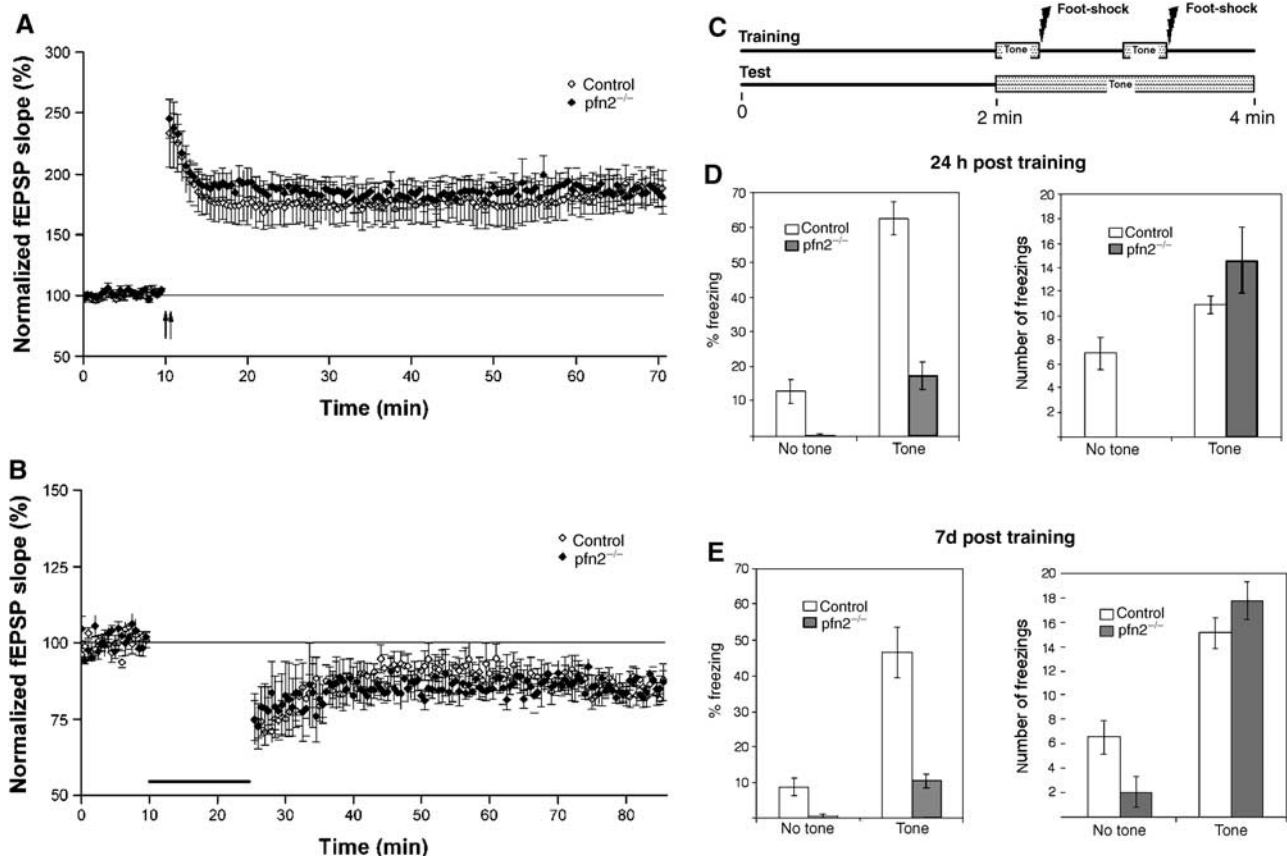


Figure 3 Synaptic plasticity, emotional learning, and memory are normal in *Pfn2*^{-/-} mice. (A) LTP and (B) LTD in *pfn2*^{-/-} mice. No differences in hippocampal long-term synaptic plasticity were observed between control and *pfn2*^{-/-} animals. The magnitude of the LTP measured between 50 and 60 min after the tetanization was 184.14 ± 12.25% in control animals (*n* = 8/3 slices) and 187.88 ± 11.98% in *pfn2*^{-/-} mice (*n* = 7/3); *P* = 0.932, ANOVA. The values of LTD were 85.09 ± 2.61% for control mice (*n* = 9/4) and 85.44 ± 0.66% for *pfn2*^{-/-} mice (*n* = 6/3); *P* = 0.917, ANOVA. (C) Outline of the performed fear conditioning experiment. (D) Twenty-four hours post training, the total freezing time in percent (left graph) and the number of freezings (right graph) were determined for *pfn2*^{-/-} (*n* = 9) and control (*n* = 9) littermates. The freezing time and the number of freezings increased during tone presentation in mutants and control mice, indicating associative learning in both groups. (E) Seven days post training, the same pattern as in (D) was observed showing no impairment of long-term memory in *pfn2*^{-/-} mice. Error bars represent s.e.m.

ments in the hippocampus were indistinguishable from control littermates (Figure 3A and B).

Also, learning and memory were normal in *pfn2*^{-/-} mice, using a fear conditioning paradigm (LeDoux, 2000) that was previously reported to involve profilin (Lamprecht *et al*, 2006). There is considerable evidence that the acquisition and retention of fear-conditioned learning is linked to plasticity in the amygdala (LeDoux, 2000). Briefly, in a training session, mice were allowed to associate a tone (conditioned cue) with a concurrent overlapping mild electrical foot-shock (unconditioned cue) (Figure 3C). Twenty-four hours later, the mice were placed in the testing chamber with altered context. The baseline freezing, as elicited by the novel environment (no tone), was first determined, followed by measuring the freezing time when the conditioned cue was presented (Figure 3D). The same test repeated 7 days later addressed whether the long-term memory of the aversive experience was maintained (Figure 3E).

Several conclusions can be drawn from the results. First, *pfn2*^{-/-} mice learned perfectly well to associate the cue with the foot-shock, as shown by the 50-fold increase in freezing time over baseline compared with the six-fold increase seen in the control mice (Figure 3D, left). Second, *pfn2*^{-/-} mice showed greatly increased motor activity when transferred to the test environment, which explains the reduced absolute freezing times. The high baseline activity of *pfn2*^{-/-} mice had a strong exploratory component, as indicated by the increased wall rearing behavior (data not shown). In order to compensate for the hyperactivity component, we deter-

mined the number of freezings instead of the total freezing time (Figure 3D and E, right graphs). After presentation of the cue (tone) the number of freezings was comparable in mutant and control mice, again demonstrating that profilin2 is not required for learning. After 7 days the same pattern of association was seen, indicating that memory had been perfectly maintained in control as well as mutant mice (Figure 3E).

Receptor clustering is another important aspect of post-synaptic activity, and profilin2 was shown to bind to gephyrin, a postsynaptic scaffolding protein involved in glycine receptor clustering (Giesemann *et al*, 2003). Experiments performed in the spinal cord of *pfn2*^{-/-} mice did not reveal any impairment of gephyrin or glycine receptor clustering (Supplementary Figure 3A), demonstrating that profilin2 is not required for arrangement of inhibitory receptors. EM immunogold studies performed in the CA1 region of the hippocampus showed that also the presentation of excitatory receptors such as NMDA and AMPA receptors was normal in *pfn2*^{-/-} mice (Supplementary Figure 3B).

Together, these data show that profilin2 is dispensable for postsynaptic activities relating to synaptic plasticity, associative learning, and memory, as well as receptor presentation.

Pfn2^{-/-} mice are hyperactive and show increased novelty-seeking behavior

The most striking phenotype of *pfn2*^{-/-} mice was the hyperexcitability in response to changes in the environment. We therefore aimed to characterize this aspect of behavior

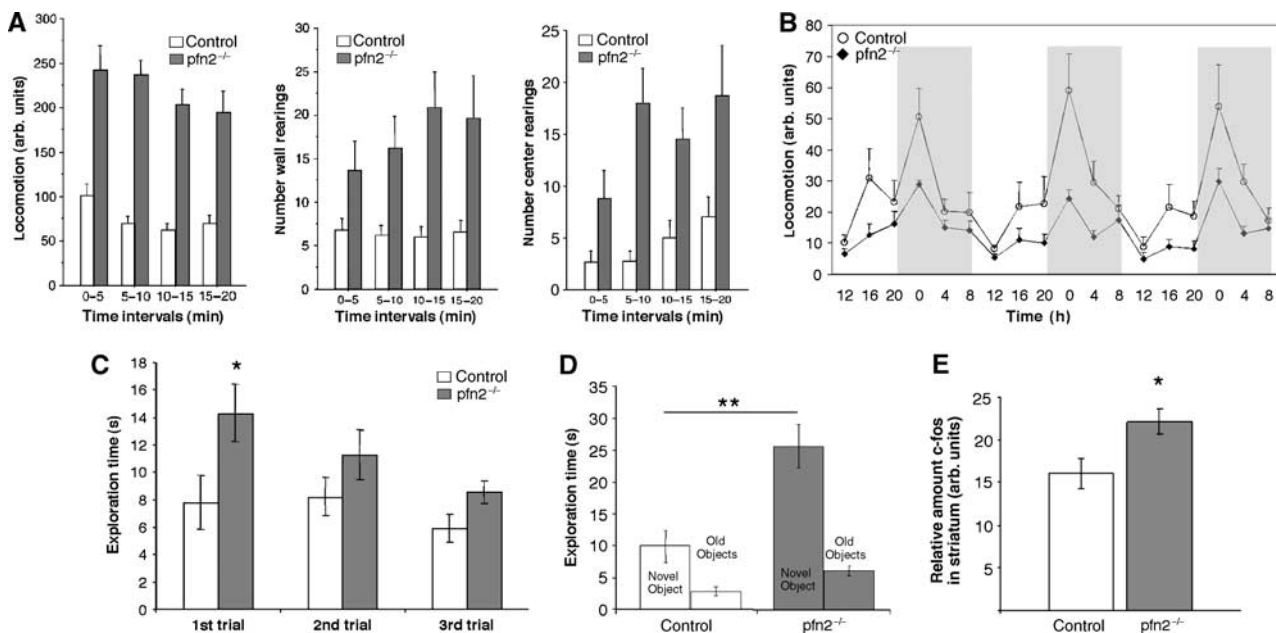


Figure 4 *Pfn2*^{-/-} mice show increased exploratory and novelty-seeking behavior as well as hyperactivation of the striatum. (A) In an open arena, *pfn2*^{-/-} mice showed increased locomotor activity (left, control *n* = 11; *pfn2*^{-/-} *n* = 11; repeated-measure ANOVA, main effect of genotype: $F[1,20] = 61.382, P < 0.0001$), wall rearings (middle), and center rearings (right, main effect of genotype: $F[1,20] = 9.431, P = 0.0060$ and $F[1,20] = 10.59, P = 0.0040$, respectively). (B) Home cage activity of *pfn2*^{-/-} mice (control *n* = 10, *pfn2*^{-/-} *n* = 9; main effect of genotype: $F[1,17] = 14.552, P = 0.0014$) kept on a 12 h dark-light cycle was reduced. (C, D) Novel object exploration test of *pfn2*^{-/-} mice (control *n* = 8, *pfn2*^{-/-} *n* = 8). In the first three trials (C) *pfn2*^{-/-} mice showed increased visits and habituation to the objects (repeated measure ANOVA, main effect of trials: $F[2,28] = 10.536, P = 0.0004$; Fisher's PLSD *post hoc* test in the first trial $P = 0.0404$. Interaction genotype \times trials: $F[2,28] = 3.215, P = 0.0554$). In trial 4 (D), replacement of an old object by a novel object leads to a significantly higher exploration in the *pfn2*^{-/-} group compared with control littermates (main effect of genotype for the exchanged object: $F[2,28] = 8.435, P = 0.0071$; Fisher's PLSD *post hoc* test on the exchanged object $P = 0.0021$). (E) c-Fos activation in the striatum of *pfn2*^{-/-} mice upon exposure to an OF arena measured by western Blot indicated higher cellular activity (*n* = 6 for each genotype; Student's *t*-test $P = 0.0269$; * $P < 0.05$, ** $P < 0.01$, *** $P < 0.001$). Error bars represent s.e.m.

and to determine the cellular and molecular mechanisms linking profilin2 and behavior.

When placed in a novel environment such as an open field (OF) arena, *pfn2*^{-/-} mice displayed increased locomotion compared with control littermates (Figure 4A, left). Increased locomotor activity was accompanied by higher stereotypic exploratory behavior such as wall rearings and center rearings (Figure 4A, middle and right). In order to determine whether knockout mice also showed hyperactivity in a familiar environment, locomotion of knockout and control littermates was monitored in the home cage. Under these conditions, knockout mice displayed significantly reduced locomotor activity (Figure 4B). Importantly, circadian rhythm, as measured by gross activity, was normal in knockout animals (repeated-measure ANOVA, interaction genotype × time: $F[17,289] = 1.352$, $P = 0.1599$). These observations confirmed that *pfn2*^{-/-} mice have increased exploratory activity in response to novelty. In order to assess whether exploratory behavior was a component contributing to the novelty-induced hyperactivity, we subjected knockout and control littermates to the novel object exploration test (Usiello *et al*, 1998; Mele *et al*, 2004). Mice were first habituated to an arena containing five objects of different shape. In the first session, *pfn2*^{-/-} mice showed significantly more visits to the objects than control animals, an effect that diminished in sessions 2–3 (Figure 4C). Control littermates showed no significant habituation, which is in agreement with previous findings for the C57 BL/6 genetic background (Roulet *et al*, 1997). Following exchange of one object for another object of different shape in session 4, *pfn2*^{-/-} mice responded with greatly increased exploration of the novel object compared with control animals (Figure 4D). These

findings are consistent with greater novelty-seeking behavior in mice lacking profilin2.

Increased synapse size and number of perforated synapses correlate with hyperactivation of the striatum in *pfn2*^{-/-} mice

Locomotor and exploratory behaviors are mediated by the striatum through the combined action of dopaminergic input and glutamatergic modulation on medium spiny neurons (for a review see West *et al*, 2003). Novel object recognition is thought to involve complex neuronal circuits, including the perirhinal cortex in rodents (Winters and Bussey, 2005), the hippocampus in monkeys (Murray and Richmond, 2001), and the anterior temporal cortex in humans (Price *et al*, 1996). However, recently it has been recognized that in rodents also the striatum is critical for mediating novelty-seeking behavior (Roulet *et al*, 2001; Bisagno *et al*, 2002), and pharmacological experiments in mice have provided evidence that glutamate signaling is important for the response to novel objects (Roulet *et al*, 2001; Sargolini *et al*, 2003). We therefore tested whether in *pfn2*^{-/-} mice an enhanced glutamatergic input contributed to hyperactivation of the striatum, as suggested by the upregulation of the immediate early marker *c-fos* (Konkle and Bielajew, 2004) in the striatum of *pfn2*^{-/-} mice exposed for 15 min to an OF arena (Figure 4E).

Ultrastructural analysis of the striatum showed that the number and overall shape of excitatory synapses was not affected in *pfn2*^{-/-} mice (Figure 5A and C). However, we observed a 20% shift in the length distribution of the active zones toward higher values (Figure 5B), as well as a 30% increase in the number of perforated synapses and multiple site boutons (Figure 5C). Changes in size and shape of

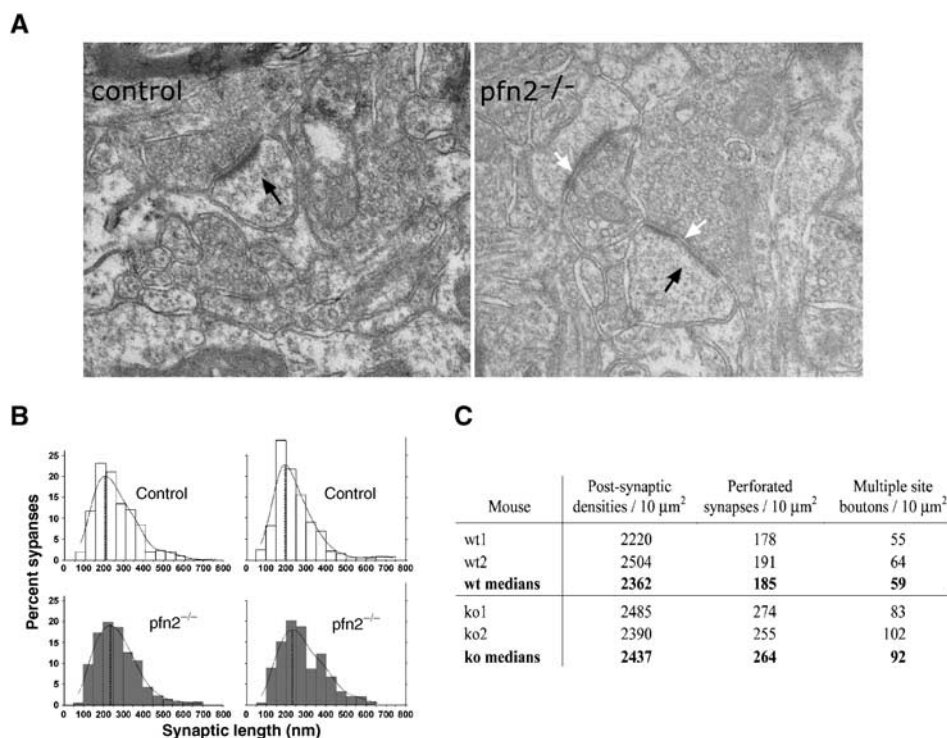


Figure 5 Increased number of perforated synapses and multiple site boutons in *pfn2*^{-/-} striata. (A) Axospinous synapses of striatum (black arrows) showed comparable ultrastructure in *pfn2*^{-/-} and control animals, but PSD length and perforations were increased in *pfn2*^{-/-} animals (white arrows). (B) The active zone lengths distribution of asymmetric synapses in the striatum was determined in two control (top) and *pfn2*^{-/-} (bottom) mice. The probability density distribution of the active zone lengths showed a shift by 40 nm to larger synapses in *pfn2*^{-/-} mice. (C) The total number of synapses is comparable, while perforated and multiple site boutons are increased by 30% in *pfn2*^{-/-} mice.

asymmetric synapses were shown to result from stimulations of excitatory neurons by environmental factors such as associative learning, or other manipulations (Geinisman *et al*, 2001), suggesting an alteration in presynaptic function in *pfn2^{-/-}* mice. To address this possibility, we focused on the physiology of the cortico-striatal glutamatergic pathway.

Profilin2 controls synaptic vesicle exocytosis

Electrophysiological currents were recorded from striatal medium spiny neurons using whole-cell patch-clamp techniques (see Materials and methods). Miniature excitatory postsynaptic currents (mEPSCs) showed no difference in the amplitude distribution (Figure 6A) and the average amplitude of the recorded events, indicating that under these conditions vesicle loading and postsynaptic response to glutamate are not altered in *pfn2^{-/-}* mice. Interestingly, the frequency of the miniature events was slightly higher in the mutant neurons ($P=0.037$ in the Kolmogorov-Smirnov test, data not shown), indicating the release of an increased number of vesicles. The higher mEPSC frequency was not due to an increased number of synapses in the striatum of *pfn2^{-/-}* mice, as shown by the synapse counts in the striatum (see Figure 5C), and the unchanged synaptic content, using synaptophysin and VGluT1 as markers (Figure 6B). A similar increase in the frequency of events was also observed for spontaneous EPSCs (Figure 6C and D, left). We then recorded spontaneous EPSCs after application of 4-aminopyridine (4-AP) to evaluate synaptic transmission under conditions of increased excitability of presynaptic afferents. In the presence of 4-AP we detected an even stronger increase of sEPSCs in *pfn2^{-/-}* neurons (Figure 6C and D, right). Taken together, these results demonstrate that presynaptic excitability is higher in *pfn2^{-/-}* mice. To further characterize the hyperexcitability under more physiological conditions, we analyzed the evoked vesicle release, while modulating the potassium and calcium concentration in the extracellular medium. Changes in K^+ concentration did not yield significant results, but in response to increased Ca^{2+} concentrations, mutant neurons released more vesicles than control neurons (Figure 6E). The increased sensitivity to Ca^{2+} entry suggested a link between the excitability phenotype and the vesicle release machinery, possibly because of changes in the vesicle release probability. To address this important parameter, we performed a paired-pulse facilitation (PPF) experiment. From 10 to 50 ms paired-pulse intervals under standard ionic conditions (1 mM Mg^{2+} , 2 mM Ca^{2+}), the PPF value for *pfn2^{-/-}* mice was significantly lower than for control littermates (Figure 6F), indicating a higher vesicle release probability in the mutants. As release probability directly correlates with the readily releasable pool size, our data suggest that profilin2 is controlling steps during vesicle docking, priming, or fusion processes (Dobrunz and Stevens, 1997). To test this directly, we used a biochemical approach based on the fraction of vSNARE bound to tSNARE at a given time. Priming of vesicles was shown to be mediated by the interaction of a vSNARE on the vesicle side and tSNAREs on the plasma membrane (Murthy and De Camilli, 2003). We immunoprecipitated tSNARE (syntaxin1) from striatal synaptosomes and found a 30% increase of complexed vSNARE (synaptobrevin2) in *pfn2^{-/-}* mice compared with control mice (Figure 7A), confirming a higher content of docked/primed vesicles in knockout mice. A similar result was

obtained by EM studies that showed a 23% increase in the number of physically docked vesicles in mutant synapses (Supplementary Figure 3C).

These alterations were not due to changes in the composition of the vesicle recycling machinery, as shown by the normal synaptic content of diverse synaptic vesicle markers in striatal synaptosomes (Figure 7B). Our data provide evidence that profilin2 acts through a mechanism that directly regulates the dynamic aspects of vesicle exocytosis.

Profilin2 regulates fast actin polymerization at the synapse

Mutations in the vesicle trafficking machinery (e.g. synapsin, Munc13-1, synaptojanin) lead to a reduction of synaptic transmission, while removal of profilin2 has the opposite effect. It is conceivable that profilin2 is controlling exocytosis via modulating the synaptic actin cytoskeleton. The mechanisms by which actin regulates exocytosis are still debated and range from providing a scaffold to tether regulatory molecules (Sankaranarayanan *et al*, 2003) to the setup of a physical barrier (Trifaro *et al*, 2002). Thus profilin2-regulated actin polymerization could be required to restrict vesicle release.

To test this possibility, we measured the ratio of F- to G-actin in cortical synaptosomes (see Materials and methods). Under resting conditions, no difference was seen in F/G-actin ratios in *pfn2^{-/-}* mice and control littermates (Figure 7C). However, stimulation of vesicle exocytosis with 20 mM KCl for 60 s resulted in a significant increase in F-actin levels in control but not knockout synaptosomes (Figure 7C). These results suggest that profilin2 is required to induce rapid actin polymerization during sustained synaptic depolarization.

Interestingly, profilin1 cannot replace profilin2 in this function. There is no trivial explanation for this specificity, and we hypothesize that distinct profilin1- and profilin2-dependent pathways exist to promote actin polymerization in the different neuronal compartments. Previous work suggested that profilin2 can bind to the WAVE-complex (Witke *et al*, 1998), which together with the Arp2/3 complex (Pollard and Borisy, 2003; Steffen *et al*, 2004) is important for site-directed actin nucleation. Binding of profilins to WAVE seems to be required for this activity (Miki *et al*, 1998).

We observed that the WAVE-complex is abundant in synaptosomes, and particularly enriched in the presynaptic matrix and the PSD (Figure 7D). Since both profilin2 and WAVE1 are associated with the presynaptic matrix (Figures 1C and 7D), the WAVE-profilin complex might play a role in directing actin nucleation to the synaptic scaffold. We therefore performed immunoprecipitation experiments from synaptosomes, which confirmed the tight interaction of profilin2 and WAVE1 in this compartment (Figure 7E). Profilin1 on the other hand does not associate with the WAVE-complex, as shown by the selectivity of WAVE binding to profilin2 but not profilin1-coupled beads (Figure 7F). These results suggest that profilin2 and WAVE cooperate in driving fast actin polymerization in the synapse, and that this pathway is different from the one used by profilin1 to promote actin polymerization.

Discussion

Ample evidence has been provided for a role of actin in presynaptic activities such as neurotransmitter release as well

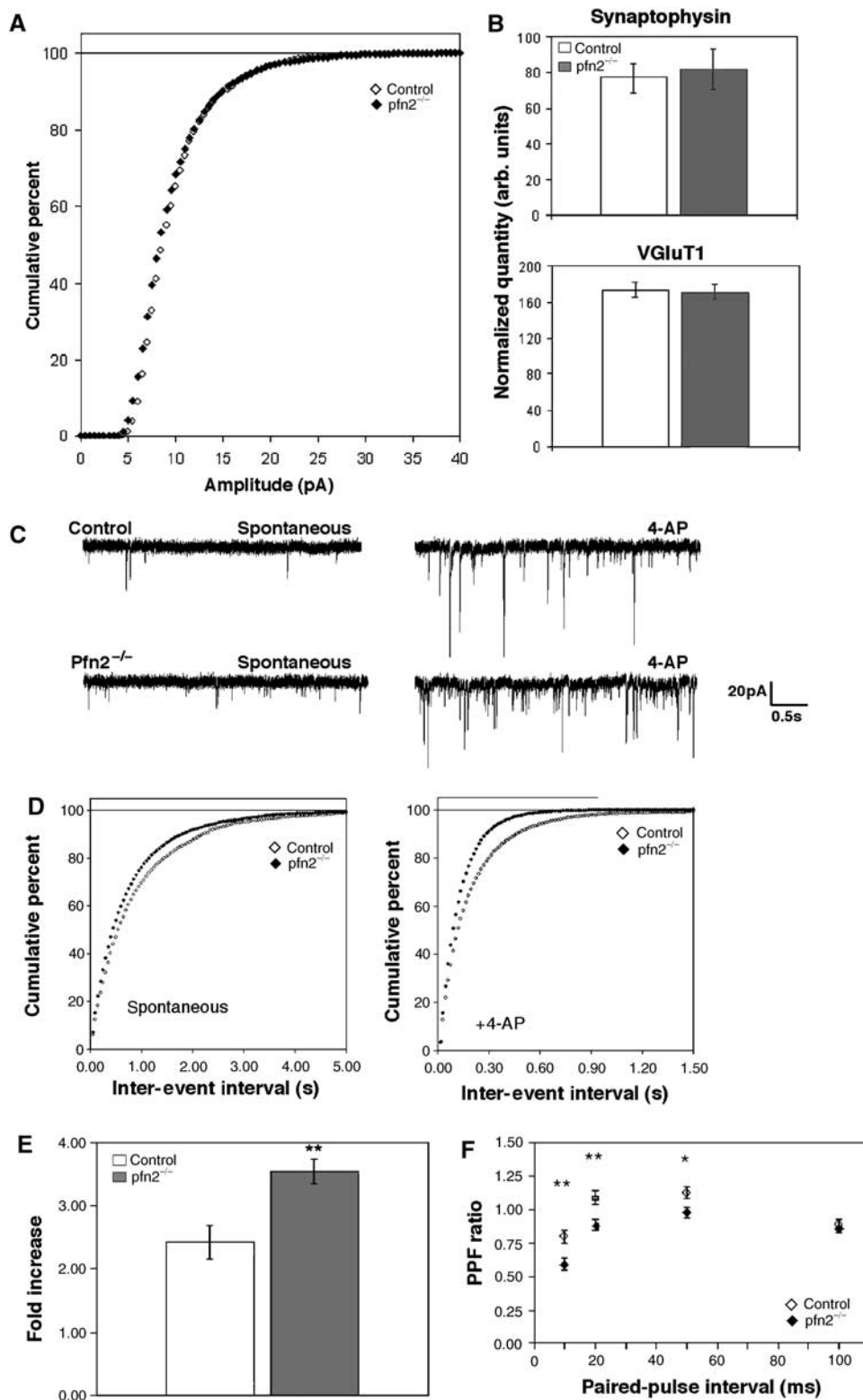


Figure 6 Glutamatergic neurons in pfn2^{-/-} mice are hyper-excitable and show higher vesicle release probability. (A) Cumulative percentage curves of the amplitude distribution of miniature EPSCs in pfn2^{-/-} ($n = 7/3$: number of cells/number of mice) and control neurons ($n = 5/3$). (B) Quantification of synaptophysin and VGLUT1 levels (synaptic content) in striata by Western blot ($n = 6$ for each genotype). (C) Representative traces from a control and a pfn2^{-/-} neuron before and after application of 4-AP illustrate the hyper-excitability of the mutant neurons. (D) Cumulative percentage curves of the average inter-event interval distribution of spontaneous EPSCs in basal conditions (spontaneous) and after application of 4-AP (+4-AP, control $n = 8/3$, pfn2^{-/-} $n = 7/2$; Kolmogorov-Smirnov test $P = 0.037$ and $P < 0.0001$, respectively). (E) Excitability of pfn2^{-/-} neurons in response to calcium increase. Evoked vesicle release upon change of $[Ca^{2+}]/[Mg^{2+}]$ ratio from 1 to 4 increased the response amplitude 3.5-fold in pfn2^{-/-} neurons, while in control neurons the increase was 2.4-fold ($P = 0.0055$ in Student's t -test; $n = 5/3$ for control and $n = 5/4$ for pfn2^{-/-} mice). (F) PPF in control and pfn2^{-/-} littermates. Pfn2^{-/-} neurons showed stronger depression that correlates with a higher release probability at presynaptic sites ($n = 10/5$ for control and $n = 11/4$ for pfn2^{-/-} mice). * $P < 0.05$, ** $P < 0.01$, *** $P < 0.001$. Error bars represent s.e.m.

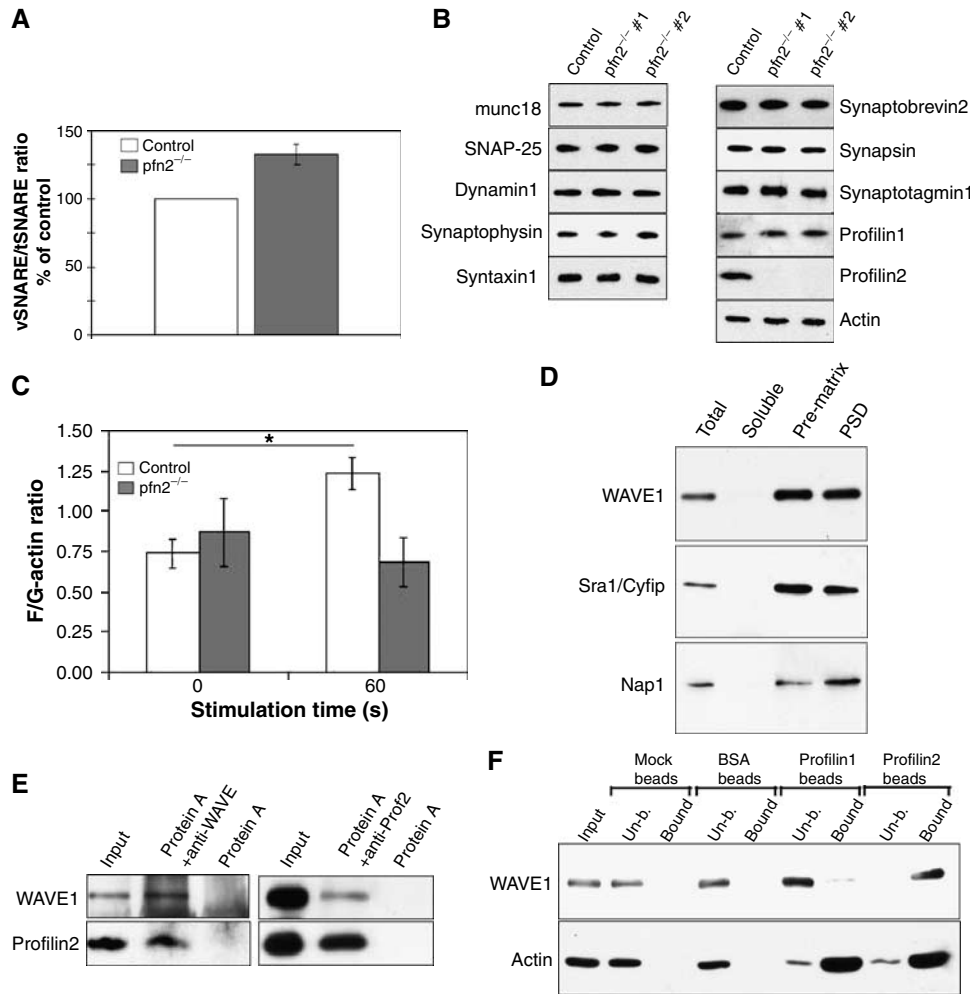


Figure 7 Lack of actin polymerization in pfn2^{-/-} synaptosomes correlates with increased vesicle docking/priming. Specific binding of the WAVE-complex to profilin2. (A) Synaptic vesicle priming based on vSNARE/tSNARE ratios after immunoprecipitation of tSNARE (syntaxin1) from pfn2^{-/-} synaptosomes is increased by 30%. vSNARE/tSNARE ratios from control mice ($n = 5$) were set to 100% and the mutant ratios ($n = 4$) expressed accordingly. (B) Synaptosomes from control and pfn2^{-/-} mice were analyzed by Western blot using a panel of antibodies detecting different markers of the vesicle release machinery. Two different mutant mice are shown to account for sample variability. (C) Synaptic F/G-actin ratios were not significantly different in resting synaptosomes (0 s), after 60 s stimulation with 20 mM K⁺ the F-actin/G-actin ratio raised in the control, while no significant increase was seen in the mutants ($n = 3$ for mutant and control; ANOVA, interaction genotype x KCl stimulation: $F[1,8] = 5.365$, $P = 0.049$). (D) Distribution of WAVE-complex components in synaptosomal fractions. WAVE1, Sra1/Cyfp, and Nap1 were found enriched in the presynaptic matrix and the PSD. (E) In synaptosomal lysate, profilin2 co-immunoprecipitated with WAVE1 (left panel) and WAVE1 co-immunoprecipitated with profilin2 (right panel). (F) Specific binding of WAVE1-complex to profilin2. Pull down of WAVE1 from cortical protein extracts using profilin1- and profilin2-coupled beads shows specificity for profilin2.

as postsynaptic processes (for a review see Dillon and Goda, 2005). However, little is known about the mechanisms and relevance of synaptic actin polymerization *in vivo*. Our mouse model for the neuron-specific G-actin binding protein profilin2 provides the first insight into how actin dynamics might control neuronal physiology and complex behavior.

Work from a number of laboratories has established a role for profilin as a key regulator of actin polymerization. Here, we provide evidence that profilin2 is required for stimulated actin polymerization in the synapse, most likely through interaction with a larger complex usually referred to as the WAVE-complex (Eden *et al.*, 2002). Although a role for the WAVE-complex in the formation of neuronal connectivity has been proposed (Pilpel and Segal, 2005), a role for WAVE-profilin interaction in synaptic actin polymerization has not been studied yet.

The *in vivo* function of profilin2 has remained enigmatic, although work on cultured neurons had suggested that profilin2 might play a role in dendritic spine stabilization and synaptic plasticity (Ackermann and Matus, 2003). Our results clearly show that LTP and LTD, as well as learning and memory, are normal in pfn2^{-/-} mice. These results do not exclude a postsynaptic role of profilin2 *per se*, but whatever this role might be, it is marginal *in vivo* when compared to the predominant presynaptic function.

The biochemical data, electrophysiology, and the EM studies presented here are all consistent with a presynaptic role of profilin2 in controlling neurotransmitter release and neuronal excitability. Loss of profilin2 leads to increased glutamate release in neocortical glutamatergic neurons and hyperstimulation of the basal ganglia, which correlates with hyperactivity and increased novelty-seeking behavior.

How does profilin2 then regulate neurotransmitter release, and how does this relate to synaptic actin polymerization? Structure, morphology, and synaptic content of synapses were comparable in mutant and control mice, but the number of primed vesicles was increased in *pfn2*^{-/-} mice, as shown by the biochemical assays and EM studies. Release probability can also be influenced by alterations in Ca²⁺ sensitivity; however, the coincidence of a roughly 30% increase in the number of primed vesicles and comparable changes in the electrophysiology suggests that mainly alterations of the readily releasable vesicle pool size contribute to the increased release probability in *pfn2*^{-/-} mice. Hence, under normal conditions, profilin2 has an inhibitory role on vesicle exocytosis.

Absence of profilin2 impairs synaptic actin polymerization and leads to an increase in the frequency of mEPSCs and evoked EPSCs similar to the one reported from experiments where actin polymerization was blocked with latrunculin (Morales *et al*, 2000; Shupliakov *et al*, 2002). Therefore, an increase of F-actin contemporary to neurotransmitter release seems to be required to provide a barrier function and to limit further vesicle exocytosis. However, we cannot exclude that also actin-independent activities of profilin2 contribute to vesicle exocytosis, since profilin2 can inhibit membrane trafficking through molecules like dynamin1 (Gareus *et al*, 2006). Other profilin2 ligands like Piccolo (Fenster *et al*, 2000) might participate in a similar way.

Another interesting aspect of profilin function in neurons is that migration, neurite extension, and cell polarization are independent of profilin2 activity, while synaptic actin polymerization cannot be rescued by profilin1. This also implies that profilin1 is the isoform that most likely regulates actin dynamics in neuronal development. The early embryonic lethal phenotype of profilin1-null mutants is in agreement with such a general role (Witke *et al*, 2001). Furthermore, the developmental defects observed in brains of heterozygous profilin1 mutant mice indicate that even subtle changes in profilin1 levels can change motile responses, while complete deletion of the more abundant profilin2 has no such effect. This again strongly suggests that in neurons profilin1 and profilin2 serve distinct functions.

Deciphering the different pathways used by profilin1 and profilin2 to control actin polymerization in neurons will be an important next step to better understand the basis of neurotransmission. Our data highlight two parameters that might contribute to the specificity of profilin1 and profilin2 in neurons—the subcellular localization and the association of profilins with different complexes. Here, we show that in neurons, members of the WAVE-complex, Nap1, Cyfip/Sra1, and WAVE1 itself, associate with profilin2 but not profilin1. We further show that the WAVE1-complex is associated with the presynaptic matrix, where also profilin2, but not profilin1 can be found. These results suggest that the WAVE1–profilin2 interaction at the synapse could be an important step in controlling actin polymerization and ultimately vesicle release. At this juncture we cannot judge the role of other actin nucleating complexes such as the formins and the Arp2/3 complex in neuronal physiology, but it is tempting to speculate that these complexes might use profilin1 to regulate neuronal migration and brain development.

In conclusion, our work shows a novel role of the actin binding protein profilin2 in brain in controlling vesicle

release, neuronal excitability, and ultimately complex behavior. The benefits of such an inhibitory effect of profilin2 could be to provide neurons with a means to better control stochastic exocytosis and to increase the dynamic range of neurotransmitter release upon stimulation. In most cell types, fine tuning of vesicle exocytosis might not be critical, but in neurons, tight and fast control of neurotransmitter release is essential. This would also explain why profilin2 is specifically expressed in cells of neuronal origin. In our mouse model, we depleted profilin2 in the entire brain and it is likely that the defects in synaptic vesicle exocytosis are not limited to cortico-striatal neurons. In fact, we have observed a similar hyperactivation of excitatory synapses in the cerebellum, which results in an age-dependent phenotype different from the one described here (P Pilo Boyl, unpublished observation).

To date no profilin2 mutations in humans have been described, and it will be interesting to see if for example SNPs can be identified and correlated with certain neurological disorders. Since profilin2 is neuron specific, it provides an excellent target to regulate actin polymerization in the synapse and thereby modulate neurotransmitter homeostasis.

Materials and methods

Histology

Animals (6–8 weeks old) were used for histological analysis. Antibody staining was performed either on frozen sections or rehydrated paraffin sections. *In situ* hybridization was performed as previously described, using the coding region of profilin1 and profilin2 to generate RNA probes (Gurniak *et al*, 2005).

Electron microscopy

Pfn2^{-/-} and control littermates (8 weeks old) were perfused with 4% paraformaldehyde and 2% glutaraldehyde in phosphate buffer (0.1 M PB, pH 7.4). The brains were postfixed in 1% OsO₄ in 0.1 cacodylate buffer, dehydrated, and embedded in epoxy resin. Synapses (PSDs of asymmetric synapses) were counted by a naive observer in the striatum of two knockout and two control brains in 100 sampling fields. Active zone sizes were measured using the MetaMorph software. We measured PSD lengths and estimated the probability density function by applying the Parzen window density estimation method, using Gaussians as the windowing functions. The density of asymmetric synapses in CA1 stratum radiatum of three mutant and three control animals was counted by naive observers for an area of 624 μm². For immunogold labeling, brain specimens from control and *pfn2*^{-/-} mice were freeze-substituted with methanol and embedded in Lowicryl HM20. Ultra-thin sections were incubated with the profilin2 antibody (for details see Sassone-Pognetto and Ottersen, 2000).

Behavior analysis

All behavior experiments were performed on male littermates from heterozygous profilin2 mutant breeding pairs that had been backcrossed seven times to C57Bl/6. All studies were conducted according to Italian national laws and regulations on the use of animals in research. *Fear conditioning*: Cue fear conditioning was performed as described in Lu *et al* (1997), with slight modifications (Lu *et al*, 1997). Briefly, in the 4 min training session after 120 s of habituation, two 20-s tone stimuli (CS) were applied, ending with a 1 s foot-shock (US, 0.4 mA), with an inter-tone interval of 40 s. Testing was performed after 24 h and 7 days in a 4 min session composed of 120 s of habituation and 120 s of tone presentation during which freezing and activity were assessed. *Home cage behavior*: Home cage locomotion and circadian rhythms were assessed using the Inframot (TSE, model 302015). *OF arena*: A standard circular white OF arena (60 cm diameter) was used in 600 lux white light conditions. Locomotion was assessed using the TSE VideoMot2 system; wall rearing and center rearing were counted manually. *Novel object exploration*: Exploration

was assessed as previously described (Usiello *et al*, 1998). Briefly, littermates were tested in an OF arena in 60 lux red light conditions. After one exploratory session in the empty arena, mice were exposed to five different objects in three consecutive 6 min sessions. After the third trial, one of the five objects was exchanged with a novel object different in shape. Exploration of the novel object as well as the old objects was scored.

Hippocampal neuron cultures

Hippocampal neurons were isolated, cultured, and analyzed as previously described (Dotti *et al*, 1988).

Biochemistry

Tissue extracts from brain were prepared by homogenizing fresh tissues in ice-cold lysis buffer (20 mM HEPES pH 7.2, 50 mM NaCl, 5 mM MgCl₂, 0.5% Tween-20 and EDTA-free protease inhibitors, Complete, Roche) using a tight fitting Douncer. Antibodies used were as follows: c-fos (Sigma), munc18 (BD Transduction Lab.), dynamin1 (Upstate), syntaxin1, synaptobrevin2, synaptotagmin (Synaptic Systems) and synapsin1 (Chemicon). *Synaptosomal fractionation*: Preparation of synaptosomes and fractionation into soluble extrasynaptic, presynaptic matrix, and PSD was carried out on dissected cortices, as previously described (Phillips *et al*, 2001). Antibodies used for synaptic markers: Synaptophysin (Sigma), SNAP-25 (Sigma) and PSD-95 (Upstate). *Synaptosomes preparation and stimulation*: Preparation of resting synaptosomes was carried out as previously described (Lopes *et al*, 1999). The synaptosomes were resuspended in HEPES-Krebs buffer, divided in aliquots, equilibrated at 37°C for 5 min, and lysed directly or after stimulation with 20 mM KCl for 60 s by adding an equal volume of 2 × PHEM extraction buffer (120 mM PIPES, 40 mM HEPES, 20 mM EGTA, 4 mM MgCl₂, 2% Triton X-100, pH 7.0). After incubation on ice for 15 min, F-actin was pelleted by a 10 min centrifugation at 100 000 r.p.m. and the supernatant (G-actin) separated. Actin was quantified by Western blot using an anti-actin antibody (MP Biochemicals). *Immunoprecipitation*: Synaptosomes were lysed in 150 mM NaCl, 50 mM Tris/HCl pH 8.0, 1% Triton X-100, and cleared by centrifugation. The supernatant was incubated with the antibody over night at 4°C and then 2 h with protein A or G beads. Antibodies for WAVE1 (BD Transduction Lab.) and Nap1 (Upstate) were purchased, antibodies for profilin2 and profilin1 were described before (Witke *et al*, 1998), monoclonal antibodies for Cyfip were raised against recombinant protein (mab5C9). *Pull-down assay*: Cortex lysates were prepared as described and then incubated with mock beads, BSA-, profilin1-, or profilin2-coupled beads. After extensive washing, bound proteins were eluted with 1 × SDS sample buffer.

Electrophysiology

Whole-cell patch recordings were performed on medium spiny neurons (anatomical and current-clamp identification) in 300–350 μm thick sagittal brain slices of 21–28-day-old pfn2^{-/-} and control littermates with an HEKA EPC9 amplifier. Miniature EPSCs were recorded in the presence of 0.5 μM tetrodotoxin (TTX, Tocris). Pharmacological excitation of the neurons was induced with 100 μM 4-AP (Sigma). Field stimulations were obtained with a glass electrode filled with HEPES-buffered extracellular medium and placed in the proximity of the patched cell. For the calcium excitability protocol, 30 stimuli at 0.1 Hz were averaged for each cell

in two subsequent [Ca²⁺]/[Mg²⁺] conditions: first [Ca²⁺]/[Mg²⁺] = 0.5 mM/[Mg²⁺] = 0.5 mM, second [Ca²⁺]/[Mg²⁺] = 2 mM/[Mg²⁺] = 0.5 mM. For the PPF, 30 pulses at 0.1 Hz were averaged for each point in standard [Ca²⁺]/[Mg²⁺] conditions. All recordings were performed in voltage patch clamp with 10 μM bicucullin. Data were recorded with Pulse 8.70 software and analyzed with Axograph, PulseFit, or IgorPro software.

LTP and LTD field recordings were carried out on 4 to 6-week-old animals and 2 to 3-week-old animals, respectively. Transverse hippocampal slices (400 μm) were cut and single slices were continuously perfused at 29°C with artificial cerebrospinal fluid (ACSF) containing the following (in mM): 120 NaCl, 2.5 KCl, 2.5 CaCl₂, 1.2 MgCl₂, 26.2 NaHCO₃, 1.0 NaH₂PO₄, 11.0 glucose, bubbled with a mixture of 95% O₂/5% CO₂, pH 7.4. fEPSPs were recorded in stratum radiatum of CA1 hippocampal region. A concentric bipolar stainless steel electrode was placed in the stratum radiatum for stimulating the Schaffer collateral afferents (0.1 ms pulse duration). Test stimuli were applied with a frequency of 0.1 Hz at a stimulus intensity that elicited an fEPSP amplitude that was ~50% of maximum. Long-term potentiation (LTP) was induced by a high-frequency stimulation (HFS) consisting of two 100-Hz trains applied with an interval of 30 s; stimulus width was 0.2 ms during the trains. For long-term depression (LTD), a low-frequency tetanus consisting of 900 pairs of pulses (distant 50 ms) at 1 Hz was used. Synaptic activity was measured as the maximal slope of the rising phase of the fEPSP. Data are presented as means ± s.e.m.

Statistical analysis

In all behavioral tests, one-way ANOVA or repeated-measures ANOVA were applied to assess statistical differences. *Post hoc* test was generally Fisher's PLSD, given that data were normally distributed and variance was not significantly different for pfn2^{-/-} and control mice. The unpaired two-tailed *t*-Student's test was used when comparing only two sets of data with normal distributions. Distributions were compared with the non-parametrical Kolmogorov-Smirnov two-sample test.

Supplementary data

Supplementary data are available at *The EMBO Journal* Online (<http://www.embojournal.org>).

Acknowledgements

We thank Dr K Rajewsky and A Egert for support with ES cell injection, Dr C Gurniak for help during the initial phase of analysis, Dr H Stöfler for providing analysis software, O Mirabeau for mathematical calculations, Dr C Dotti for advice with neuron cultures, Dr M Rust for help with the profilin1 mutant mice, and C Gross for critical reading of the manuscript. This work was supported by a short-term fellowship to PPB, funding by Miur (Grant Prin #2005059123 to MS-P and Grant Prin #2005053844 to MG) and Regione Piemonte (Grant 2004 A218 to MSP). MM was supported by an 'E-STAR' fellowship (EC FP6 Marie Curie Host fellowship under contract number MEST-CT-2004-504640). HV was supported by the Spanish Ministerio de Educacion y Ciencia, grant number EX2006-0294.

References

- Ackermann M, Matus A (2003) Activity-induced targeting of profilin and stabilization of dendritic spine morphology. *Nat Neurosci* **6**: 1194–1200
- Balasubramanian MK, Hirani BR, Burke JD, Gould KL (1994) The *Schizosaccharomyces pombe* cdc3+ gene encodes a profilin essential for cytokinesis. *J Cell Biol* **125**: 1289–1301
- Bisagno V, Ferguson D, Luine VN (2002) Short toxic methamphetamine schedule impairs object recognition task in male rats. *Brain Res* **940**: 95–101
- Bradke F, Dotti CG (1999) The role of local actin instability in axon formation. *Science* **283**: 1931–1934
- Carlsson L, Nystrom LE, Sundkvist I, Markey F, Lindberg U (1977) Actin polymerizability is influenced by profilin, a low molecular weight protein in non-muscle cells. *J Mol Biol* **115**: 465–483
- Cooley L, Verheyen E, Ayers K (1992) chickadee encodes a profilin required for intercellular cytoplasm transport during *Drosophila* oogenesis. *Cell* **69**: 173–184
- Di Nardo A, Gareus R, Kwiatkowski D, Witke W (2000) Alternative splicing of the mouse profilin II gene generates functionally different profilin isoforms. *J Cell Sci* **113** (Part 21): 3795–3803
- Dillon C, Goda Y (2005) The actin cytoskeleton: integrating form and function at the synapse. *Annu Rev Neurosci* **28**: 25–55
- Dobrunz LE, Stevens CF (1997) Heterogeneity of release probability, facilitation, and depletion at central synapses. *Neuron* **18**: 995–1008

- Dotti CG, Sullivan CA, Banker GA (1988) The establishment of polarity by hippocampal neurons in culture. *J Neurosci* **8**: 1454–1468
- Eden S, Rohatgi R, Podtelejnikov AV, Mann M, Kirschner MW (2002) Mechanism of regulation of WAVE1-induced actin nucleation by Rac1 and Nck. *Nature* **418**: 790–793
- Fenster SD, Chung WJ, Zhai R, Cases-Langhoff C, Voss B, Garner AM, Kaempfer U, Kindler S, Gundelfinger ED, Garner CC (2000) Piccolo, a presynaptic zinc finger protein structurally related to bassoon. *Neuron* **25**: 203–214
- Gareus R, Di Nardo A, Rybin V, Witke W (2006) Mouse profilin 2 regulates endocytosis and competes with SH3 ligand binding to dynamin 1. *J Biol Chem* **281**: 2803–2811
- Geinisman Y, Berry RW, Disterhoft JF, Power JM, Van der Zee EA (2001) Associative learning elicits the formation of multiple-synapse boutons. *J Neurosci* **21**: 5568–5573
- Gieselmann R, Kwiatkowski DJ, Janmey PA, Witke W (1995) Distinct biochemical characteristics of the two human profilin isoforms. *Eur J Biochem* **229**: 621–628
- Gieseemann T, Schwarz G, Nawrotzki R, Berhorster K, Rothkegel M, Schluter K, Schrader N, Schindelin H, Mendel RR, Kirsch J, Jockusch BM (2003) Complex formation between the postsynaptic scaffolding protein gephyrin, profilin, and Mena: a possible link to the microfilament system. *J Neurosci* **23**: 8330–8339
- Gurniak CB, Perlas E, Witke W (2005) The actin depolymerizing factor n-cofilin is essential for neural tube morphogenesis and neural crest cell migration. *Dev Biol* **278**: 231–241
- Haugwitz M, Noegel AA, Karakesisoglou J, Schleicher M (1994) *Dictyostelium* amoebae that lack G-actin-sequestering profilins show defects in F-actin content, cytokinesis, and development. *Cell* **79**: 303–314
- Konkle AT, Bielajew C (2004) Tracing the neuroanatomical profiles of reward pathways with markers of neuronal activation. *Rev Neurosci* **15**: 383–414
- Kovar DR, Harris ES, Mahaffy R, Higgs HN, Pollard TD (2006) Control of the assembly of ATP- and ADP-actin by formins and profilin. *Cell* **124**: 423–435
- Lambrechts A, van Damme J, Goethals M, Vandekerckhove J, Ampe C (1995) Purification and characterization of bovine profilin II. Actin, poly(L-proline) and inositolphospholipid binding. *Eur J Biochem* **230**: 281–286
- Lamprecht R, Farb CR, Rodrigues SM, LeDoux JE (2006) Fear conditioning drives profilin into amygdala dendritic spines. *Nat Neurosci* **9**: 481–483
- LeDoux JE (2000) Emotion circuits in the brain. *Annu Rev Neurosci* **23**: 155–184
- Lopes LV, Cunha RA, Ribeiro JA (1999) Cross talk between A(1) and A(2A) adenosine receptors in the hippocampus and cortex of young adult and old rats. *J Neurophysiol* **82**: 3196–3203
- Lu YM, Jia Z, Janus C, Henderson JT, Gerlai R, Wojtowicz JM, Roder JC (1997) Mice lacking metabotropic glutamate receptor 5 show impaired learning and reduced CA1 long-term potentiation (LTP) but normal CA3 LTP. *J Neurosci* **17**: 5196–5205
- Mele A, Avena M, Roulet P, De Leonibus E, Mandillo S, Sargolini F, Coccarello R, Oliverio A (2004) Nucleus accumbens dopamine receptors in the consolidation of spatial memory. *Behav Pharmacol* **15**: 423–431
- Miki H, Suetsugu S, Takenawa T (1998) WAVE, a novel WASP-family protein involved in actin reorganization induced by Rac. *EMBO J* **17**: 6932–6941
- Morales M, Colicos MA, Goda Y (2000) Actin-dependent regulation of neurotransmitter release at central synapses. *Neuron* **27**: 539–550
- Murray EA, Richmond BJ (2001) Role of perirhinal cortex in object perception, memory, and associations. *Curr Opin Neurobiol* **11**: 188–193
- Murthy VN, De Camilli P (2003) Cell biology of the presynaptic terminal. *Annu Rev Neurosci* **26**: 701–728
- Neuhoff H, Sassoe-Pognetto M, Panzanelli P, Maas C, Witke W, Kneussel M (2005) The actin-binding protein profilin I is localized at synaptic sites in an activity-regulated manner. *Eur J Neurosci* **21**: 15–25
- Obermann H, Raabe I, Balvers M, Brunswig B, Schulze W, Kirchhoff C (2005) Novel testis-expressed profilin IV associated with acrosome biogenesis and spermatid elongation. *Mol Hum Reprod* **11**: 53–64
- Phillips GR, Huang JK, Wang Y, Tanaka H, Shapiro L, Zhang W, Shan WS, Arndt K, Frank M, Gordon RE, Gawinowicz MA, Zhao Y, Colman DR (2001) The presynaptic particle web: ultrastructure, composition, dissolution, and reconstitution. *Neuron* **32**: 63–77
- Pilpel Y, Segal M (2005) Rapid WAVE dynamics in dendritic spines of cultured hippocampal neurons is mediated by actin polymerization. *J Neurochem* **95**: 1401–1410
- Pollard TD, Borisy GG (2003) Cellular motility driven by assembly and disassembly of actin filaments. *Cell* **112**: 453–465
- Pollard TD, Blanchoin L, Mullins RD (2001) Actin dynamics. *J Cell Sci* **114**: 3–4
- Price CJ, Moore CJ, Humphreys GW, Frackowiak RS, Friston KJ (1996) The neural regions sustaining object recognition and naming. *Proc Biol Sci* **263**: 1501–1507
- Roulet P, Mele A, Ammassari-Teule M (1997) Ibotenic lesions of the nucleus accumbens promote reactivity to spatial novelty in nonreactive DBA mice: implications for neural mechanisms subserving spatial information encoding. *Behav Neurosci* **111**: 976–984
- Roulet P, Sargolini F, Oliverio A, Mele A (2001) NMDA and AMPA antagonist infusions into the ventral striatum impair different steps of spatial information processing in a nonassociative task in mice. *J Neurosci* **21**: 2143–2149
- Sankaranarayanan S, Atluri PP, Ryan TA (2003) Actin has a molecular scaffolding, not propulsive, role in presynaptic function. *Nat Neurosci* **6**: 127–135
- Sargolini F, Roulet P, Oliverio A, Mele A (2003) Effects of intracumbens focal administrations of glutamate antagonists on object recognition memory in mice. *Behav Brain Res* **138**: 153–163
- Sassoe-Pognetto M, Ottersen OP (2000) Organization of ionotropic glutamate receptors at dendrodendritic synapses in the rat olfactory bulb. *J Neurosci* **20**: 2192–2201
- Shupliakov O, Bloom O, Gustafsson JS, Kjaerulff O, Low P, Tomilin N, Pieribone VA, Greengard P, Brodin L (2002) Impaired recycling of synaptic vesicles after acute perturbation of the presynaptic actin cytoskeleton. *Proc Natl Acad Sci USA* **99**: 14476–14481
- Steffen A, Rottner K, Ehinger J, Innocenti M, Scita G, Wehland J, Stradal TE (2004) Sra-1 and Nap1 link Rac to actin assembly driving lamellipodia formation. *EMBO J* **23**: 749–759
- Trifaro JM, Lejen T, Rose SD, Pene TD, Barkar ND, Seward EP (2002) Pathways that control cortical F-actin dynamics during secretion. *Neurochem Res* **27**: 1371–1385
- Usiello A, Sargolini F, Roulet P, Ammassari-Teule M, Passino E, Oliverio A, Mele A (1998) N-methyl-D-aspartate receptors in the nucleus accumbens are involved in detection of spatial novelty in mice. *Psychopharmacology (Berl)* **137**: 175–183
- Wang X, Kibschull M, Laue MM, Lichte B, Petrasch-Parwez E, Kilmann MW (1999) Aczonin, a 550-kD putative scaffolding protein of presynaptic active zones, shares homology regions with Rim and Bassoon and binds profilin. *J Cell Biol* **147**: 151–162
- West AR, Floresco SB, Charara A, Rosenkranz JA, Grace AA (2003) Electrophysiological interactions between striatal glutamatergic and dopaminergic systems. *Ann N Y Acad Sci* **1003**: 53–74
- Winters BD, Bussey TJ (2005) Glutamate receptors in perirhinal cortex mediate encoding, retrieval, and consolidation of object recognition memory. *J Neurosci* **25**: 4243–4251
- Witke W, Podtelejnikov AV, Di Nardo A, Sutherland JD, Gurniak CB, Dotti C, Mann M (1998) In mouse brain profilin I and profilin II associate with regulators of the endocytic pathway and actin assembly. *EMBO J* **17**: 967–976
- Witke W, Sutherland JD, Sharpe A, Arai M, Kwiatkowski DJ (2001) Profilin I is essential for cell survival and cell division in early mouse development. *Proc Natl Acad Sci USA* **98**: 3832–3836